Title

A fully coupled ecosystem model to predict the foraging ecology of apex predators in the California Current

Authors

Fiechter, J
Huckstadt, LA
Rose, KA
et al.

Publication Date

2016-09-08

DOI

10.3354/meps11849

Peer reviewed

Vol. 556: 273–285, 2016
doi: 10.3354/meps11849

MARINE ECOLOGY PROGRESS SERIES
Mar Ecol Prog Ser

Published September 8

A fully coupled ecosystem model to predict the foraging ecology of apex predators in the California Current

J. Fiechter[1,*], L. A. Huckstadt[2], K. A. Rose[3], D. P. Costa[2]

[1]Institute of Marine Sciences, University of California Santa Cruz, 1156 High St, Santa Cruz, CA 95064, USA
[2]Department of Ecology and Evolutionary Biology, University of California Santa Cruz, 1156 High St, Santa Cruz, CA 95064, USA
[3]Department of Oceanography and Coastal Sciences, Louisiana State University, 1002-Y Energy, Coast & Environment Building, Baton Rouge, LA 70803, USA

ABSTRACT: Results from a fully coupled end-to-end ecosystem model for the California Current Large Marine Ecosystem are used to describe the impact of environmental variability and prey availability on the foraging ecology of its most abundant apex predator, the California sea lion *Zalophus californianus*. The ecosystem model consists of a biogeochemical submodel embedded in a regional ocean circulation submodel, both coupled with a multi-species individual-based submodel for forage fish (sardine and anchovy) and California sea lions. Sardine and anchovy are explicitly represented in the model as they are commonly found in the diet of sea lions and exhibit significant interannual and decadal variability in population abundances that reflect variations in their environment and lower trophic level prey. Output from a 20 yr run (1989–2008) of the model demonstrates how different physical and biological processes control habitat utilization and foraging success of California sea lions on interannual time scales, with the dominant modes of variability linked to sardine abundance and coastal upwelling intensity. The results also illustrate how variability in environmental conditions, forage fish distribution, and prey assemblage affect sea lion feeding success. While specifically focusing on the foraging ecology of sea lions, the modeling framework has the ability to provide a more complete understanding of the physical and biological mechanisms impacting trophic interactions in the California Current, or other regions where similar fully coupled ecosystem models may be implemented.

KEY WORDS: Ecosystem model · Foraging ecology · California Current · Upwelling · Sea lions · Marine predators · *Zalophus californianus*

INTRODUCTION

Determining the relationships between environmental variability, prey field dynamics, and the foraging ecology of marine mammals and other apex predators has been an on-going research topic for several decades (Fiedler et al. 1998). However, recent progress in animal tagging has shed new light on the mechanisms through which changing environmental conditions may impact the habitat selection of pelagic predators (Block et al. 2011, Irvine et al. 2014). Such information is critical to identify the underlying physical and biological processes that control the foraging and migratory behavior of higher trophic level species (Weise et al. 2006, Bailey et al. 2009). Understanding the linkages among environmental variability, prey availability, and predator distribution should ultimately lead to a better characterization of biological 'hotspots' in the ocean and how these hotspots may respond to changing climate conditions (Palacios et al. 2006).

*Corresponding author: fiechter@ucsc.edu

In coastal upwelling regions such as the California Current Large Marine Ecosystem (CCLME), small pelagic forage fish (e.g. sardine and anchovy) constitute a significant part of the diet of apex predators. Because the variability in abundance and distribution of small pelagic fish reflects spatial and temporal changes in their environment (Bakun 2006, Field et al. 2006), the foraging ecology of their predators is also expected to depend on the fundamental processes regulating ocean conditions and lower trophic level production. Environmental variability in the CCLME is seasonally tied to the coastal upwelling of cool, nutrient-rich waters in response to prevailing alongshore winds, leading to elevated levels of new primary production along the majority of the US west coast. The region between the coastal upwelling zone and the offshore oligotrophic waters of the North Pacific subtropical gyre (i.e. 100 to 300 km from the coast) is known as the California Current transition zone (CCTZ; Brink & Cowles 1991), and is primarily influenced by mesoscale processes and wind stress curl (Kosro et al. 1991). Physical and biological differences between the nearshore upwelling region and the CCTZ also determine habitat for planktivorous pelagic species, such as sardine that concentrate in the CCTZ and anchovy that favor the nearshore regions (Rykaczewski & Checkley 2008). In addition to intense seasonal upwelling and eddy activity, the CCLME also responds to known modes of regional climate variability, such as the El Niño Southern Oscillation (ENSO), the Pacific Decadal Oscillation (PDO), and the North Pacific Gyre Oscillation (NPGO) (Mantua et al. 1997, Lynn & Bograd 2002, Di Lorenzo et al. 2008).

Here a fully coupled ecosystem model is used to identify the effects of environmental conditions and prey availability on the foraging ecology (i.e. habitat utilization and feeding success) of adult male California sea lions *Zalophus californianus* off of central California (Fig. 1). The model framework consists of a regional ocean circulation submodel, a biogeochemical submodel, and a multi-species, individual-based submodel representing sardine, anchovy, and sea lions. Sea lions are the most abundant apex predator in the CCLME (Carretta et al. 2005), and their foraging behavior has been observed to shift from predominantly nearshore to farther offshore during anomalously warm conditions (Weise et al. 2006). Sardine and anchovy are specifically included in the model, as their population abundances exhibit significant interannual and decadal fluctuations (Schwartzlose et al. 1999), and they are commonly found in the diet of California sea lions (Lowry & Carretta 1999) although with a significant degree of year-to-year variability (Weise & Harvey 2008, McClatchie et al. 2016). The main focus of the present work is therefore to demonstrate that the fully coupled model can be used to track environmental and feeding conditions experienced by sea lions on daily to interannual timescales, and to investigate the complex interplay between environmentally mediated behavioral responses and prey-mediated feeding conditions as drivers for year-to-year variations in their foraging patterns and success off of central California. As such, the results provide insight into the physical and biological mechanisms impacting the foraging ecology of California sea lions in the CCLME. Since the details and simulation results of the physical submodel, biogeochemical submodel, and forage fish component of the individual-based submodel have been extensively described elsewhere (Fiechter et al. 2015, Rose et al. 2015), the emphasis is placed here on the sea lion component of the individual-based submodel and its coupling to the other submodels.

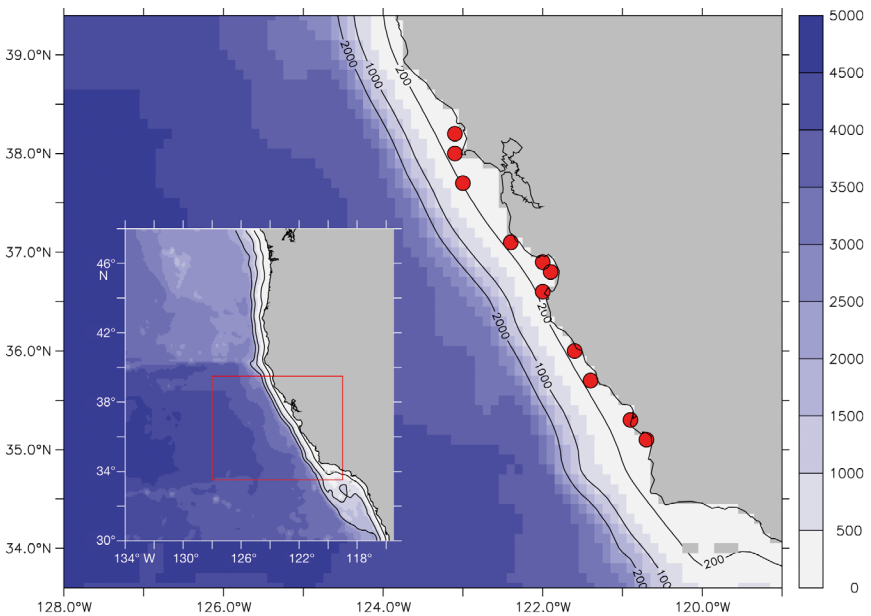

Fig. 1. Model domain for the California Current Large Marine Ecosystem (inset) and haul-out locations (red circles) identified from tracking data for California sea lions *Zalophus californianus* along the coast of central California, USA. Color scale represents bottom topography (m)

METHODS

Regional ocean circulation submodel

The ocean circulation submodel is an implementation of the Regional Ocean Modeling System (ROMS) (Shchepetkin & McWilliams 2005, Haidvogel et al. 2008) for the CCLME. The domain ranges from 30 to 48° N and 116 to 134° W (Fig. 1, inset) with a horizontal grid resolution of 1/10° and 42 terrain-following vertical levels. The ROMS submodel is forced on all lateral boundaries by monthly averaged fields from the Simple Ocean Data Assimilation reanalysis (Carton et al. 2000). Surface forcing is derived from the datasets for Common Ocean-Ice Reference Experiments (CORE2) (Large & Yeager 2009), which consist of 6-hourly atmospheric variables (wind, air temperature, sea level pressure, and specific humidity), daily short- and long-wave radiation, and monthly precipitation.

Biogeochemical submodel

The biogeochemical submodel is based on the 11-component North Pacific Ecosystem Model for Understanding Regional Oceanography (NEMURO; Kishi et al. 2007). NEMURO includes 3 limiting nutrients (nitrate, ammonium, and silicic acid), 2 phytoplankton groups (nanophytoplankton and diatoms), 3 zooplankton groups (micro-, meso-, and predatory zooplankton), and 3 detritus pools (dissolved and particulate organic nitrogen and particulate silica). Coupling to the ocean circulation is done by solving a transport equation in ROMS for each NEMURO variable in each grid cell at every time step. Boundary conditions for nutrients are based on monthly climatological values from the World Ocean Atlas (Conkright & Boyer 2002), and those for phytoplankton, zooplankton, and detritus are set to a small value. A detailed description of the NEMURO configuration and specific parameter values for the CCLME is provided elsewhere (Rose et al. 2015).

Multi-species, individual-based submodel

Since a complete description of the forage fish component of the individual-based submodel (IBM) is available elsewhere (Fiechter et al. 2015, Rose et al. 2015), only a brief overview is presented here. Specific details related to sea lion bioenergetics are also provided in the Supplement at www.int-res.com/articles/suppl/m556p273_supp.pdf.

Sardine and anchovy

The sardine and anchovy component of the IBM uses a super-individual approach (Scheffer et al. 1995), where a fixed number of model individuals are followed, and each model individual is worth some number of identical population individuals. Growth of anchovy and sardine model individuals is computed based on bioenergetics and a functional response relationship using zooplankton concentrations from the NEMURO submodel. In the model, anchovy mainly feed on larger prey types found in coastal waters, while sardine prefer smaller prey types typically found in offshore waters. Mortality acts to decrease the worth of sardine and anchovy super-individuals, and accounts for natural mortality rate, size-dependent starvation (from weight–length relationships), and dynamically imposed predation from California sea lions.

The 3-dimensional position of each sardine and anchovy super-individual is updated hourly and followed both in continuous (longitude, latitude, depth) space and ROMS grid cell location. A kinesis approach (Humston et al. 2004) with a combined cue based on temperature and prey availability is used to simulate horizontal movement of the fish, while vertical movement is simulated more simply by positioning the individuals at the depth where consumption is maximized. Optimal temperature conditions are set to 14 ± 1°C for sardine (typical of offshore waters) and 12 ± 2°C for anchovy (typical of upwelled coastal waters). The choice of optimal temperatures and tolerances is based on reported ranges for preferred growth and spawning conditions specific to sardine and anchovy (Rose et al. 2015).

California sea lion

The sea lion component of the IBM simulates the foraging ecology of adult males, where each model individual represents 1 animal (as opposed to the super-individual approach used in the fish IBM). Emphasis is placed on male sea lions primarily to avoid additional model complexity associated with simulating reproduction costs and nursing constraints on foraging for female individuals. Furthermore, the observational evidence suggesting a shift in foraging patterns during anomalous upwelling

conditions that motivated this study was exclusively based on tracking data for male sea lions (Weise et al. 2006).

Sea lion bioenergetics are represented by a mechanistic dynamic model (Lavigne et al. 1986), which separates energy demands into production and maintenance (i.e. growth is needed to maintain body mass by compensating the energy expended during foraging or resting). Because the costs associated with reproductive growth can be neglected for male mammals, the bioenergetics model simplifies to a balance between consumption, metabolism, and waste. Depending on the daily balance between the energy acquired from fish consumption and that required for production and metabolism, individual sea lions achieve either optimal growth, sub-optimal growth, or negative growth. Energy consumption is calculated on an hourly basis using an estimate of daily food intake as a function of body mass (Kastelein et al. 2000). The model assumes that sea lions feed preferentially on sardine and anchovy (from the forage fish component of the IBM), but if an individual is unable to meet its desired consumption based on these 2 species alone, the missing biomass can be acquired by feeding on 2 additional prey source (i.e. market squid and jack mackerel). Because sea lions are opportunistic feeders and have a diverse diet, it is reasonable to assume that they can on average fulfill their intake needs by combining multiple prey sources (although this probably occurs over the course of several foraging trips instead of hourly as imposed in the model for simplicity). Consumption was parameterized so that relative diet contributions (in units of biomass) were approximately 33% for anchovy, 17% for sardine, 38% for market squid, and 12% for mackerel, which roughly reflect long-term diet information from southern California (Lowry & Carretta 1999). However, existing data suggest a significant degree of spatial and temporal variability in diet composition, with sardines becoming more dominant (60–80% of diet) during El Niño conditions (Weise & Harvey 2008) or both sardine and anchovy percentages dropping (<20% of the diet) during periods of lower population abundances for these species (Hassrick et al. 2014, McClatchie et al. 2016).

Horizontal foraging movement for sea lions is simulated using kinesis (Humston et al. 2004) with optimal temperature conditions of 12 ± 2°C corresponding to the signature of recently upwelled, productive waters. Kinesis uses a combination of inertial and random displacements based on the proximity to ideal conditions, whereby inertial or random behaviors are more heavily weighted when temperatures are, respectively, near or far from optimal. Such behavior allows an individual to maintain itself in a favorable environment (inertial component) or to perform a random search for a better environment when conditions deviate too far from optimal (random component). Because sea lions typically swim near the surface while foraging and their feeding dives are short (ca. 20 min) relative to the IBM time step (1 h), vertical behavior is currently neglected and individuals are only followed horizontally using the surface layer of the ROMS grid. However, sea lions are assumed to detect sardine and anchovy individuals throughout the water column within a specified horizontal search radius based on swimming speed and model time step.

Foraging trip duration is primarily determined by feeding success, with sea lion individuals targeting to maintain a constant fat content. Since body mass decreases when they are hauled out (i.e. negative growth), losing the amount of fat stored during the previous foraging trip triggers the start of the next foraging trip. Similarly, sea lions keep foraging until they regain the fat content lost while resting, at which point they head back to land by biasing their movement towards the closest haul-out location (Fig. 1). To avoid unrealistically short foraging trips and to increase model realism, a minimum duration of 1 d is imposed for each haul-out period and foraging trip (i.e. the individuals spend at least 1 d on land before starting their next trip and stay at least 1 d at sea before returning to land). Foraging trips are also limited to a maximum of 3 d, after which sea lions start heading back towards the closest haul-out location whether or not they regained sufficient fat content. While arbitrary, these bounds on foraging and haul-out durations are meant to reflect actual tracking data from male sea lions off of California (Weise et al. 2006) suggesting that ca. 90% of foraging trips last less than 3 d and ca. 97% of haul-out periods are shorter than 2 d. More importantly, the limits imposed on behavior in the model serve the purpose of correctly reproducing the average time fraction spent by sea lions on land vs. at sea (i.e. 41% in the IBM compared to 40% in the tracking data).

Model simulation and analysis method

The fully coupled ecosystem model simulation spanned the period 1988 to 2008, which encompasses one of the strongest ENSO events on record in 1997–98, a warm-to-cold PDO regime shift in the late 1990s, and years identified as normal (2004)

and anomalous (2005) for sea lion foraging based on tracking data (Weise et al. 2006). To minimize model spin-up, initial conditions (i.e. 1 January 1988) for the physics, biogeochemistry, and sardine and anchovy component of the IBM were taken directly from an existing 50 yr simulation for the period 1959 to 2008 (Rose et al. 2015). For the sea lion component of the IBM, 1000 individuals were initialized on 1 January 1988 with a weight of 250 kg each, and randomly assigned to 1 of the 11 haul-out locations identified from tracking data for male animals off of central California (Fig. 1).The first year of the simulation (i.e. 1988) was discarded to allow for a redistribution of the sea lion individuals amongst the various haul-out locations in response to environmental conditions, leaving a 20 yr integration (1989 to 2008) of the ecosystem model for further analysis and interpretation (Fig. S1 in the Supplement).

While physical and biogeochemical variability clearly modulates sardine and anchovy population dynamics (Fiechter et al. 2015), the model analysis was focused on exploring the complex interplay between environmentally mediated behavioral response and prey-mediated feeding conditions as drivers for interannual variations in the foraging patterns and success of sea lions off of central California. An empirical orthogonal function (EOF) decomposition was used to extract dominant modes of variability, and to isolate relationships between environmental, prey, and foraging characteristics. EOF decomposition is a statistical method similar to principal component analysis, but with the advantage of identifying both spatial and temporal patterns of variability by calculating orthogonal basis functions (i.e. EOF modes) from the eigenvectors of the covariance matrix formed by the spatial (rows) and temporal (columns) values for the variable of interest (e.g. Thomson & Emery 2014). The basis functions are determined so that they sequentially account for the largest remaining amount of the total variance present in the original data, as determined by the eigenvalues of the covariance matrix (i.e. each eigenvalue represents the relative variance explained by the corresponding EOF mode). Its intrinsic properties make EOF decomposition particularly attractive for extracting patterns of variability in the full 3 dimensional (x, y, t) fields without reducing the dimensionality of the data via arbitrary spatial or temporal averaging. Because monthly variability in sea lion foraging locations in the model is predominantly associated with seasonal upwelling dynamics (i.e. the optimal temperature for behavior is that of recently upwelled waters), the analysis was rather focused on interannual fluctuations, and EOF modes were therefore determined for annual (calendar year) values of simulated sea lion abundances, sea surface temperatures (SST), and sardine and anchovy population abundances.

Using 12 h snapshots, annual sea lion abundances were calculated by summing over time the total number of individuals present in each surface grid cell, while annual mean sardine and anchovy abundances were determined by averaging over time the total number of fish individuals present in the water column below each surface grid. Annual mean SST values were obtained by averaging monthly mean temperatures for each cell. EOFs were then computed over the entire model domain, with each cell treated as a time series of 20 values. Each EOF mode was characterized by a single spatial map (in native units), a normalized annual amplitude, and the percent of the total variance explained by the mode (Fig. S2). Pearson correlations between the EOF annual amplitudes were used to determine the strength of the relationships between sea lion abundance and explanatory variables (i.e. SST and sardine and anchovy abundances). Foraging success was also summarized per calendar year using 12 h snapshots of simulated sea lion traits consisting of body mass, fat depot (i.e. a proxy for optimal growth conditions), resting time, trip duration, and diet. Non-spatial annual mean values of the traits were obtained by first averaging over all model individuals every 12 h and then averaging over all snapshots in a year. The relative importance of sardine and anchovy contributions to the diet of the sea lions was evaluated by comparing normalized changes in the annual consumption of each species with respect to the 20 yr mean.

A binary discriminator test (Stow et al. 2009) was used to assess the fidelity with which the ecosystem model reproduced sea lion satellite tracking data available for 2003 to 2006, namely whether observed animal locations could be reliably predicted from simulated foraging patterns. Model skill was quantified in terms of presence predictive value (PPV), absence predictive value (APV), and combined predictive value (CPV):

$$\begin{aligned} \mathrm{PPV} &= \frac{\mathrm{TP}}{\mathrm{TP}+\mathrm{FP}} \\ \mathrm{APV} &= \frac{\mathrm{TN}}{\mathrm{TN}+\mathrm{FN}} \\ \mathrm{CPV} &= \frac{\mathrm{TP}+\mathrm{TN}}{\mathrm{TP}+\mathrm{TN}+\mathrm{FP}+\mathrm{FN}} \end{aligned} \quad (1)$$

True positive (TP) and true negative (TN) values mean that the model correctly predicted presence or absence of an actual sea lion, while false positive (FP)

Table 1. Pearson correlation coefficients for the first and second empirical orthogonal function (EOF) modes of California sea lion (CSL) annual abundances and annual mean fat depot against explanatory variables (first and second EOF modes for annual mean sea surface temperature [SST] and sardine and anchovy abundances). The strongest correlations between explanatory variables and sea lion mode 1 (0.75, $p < 0.01$), mode 2 (0.73, $p < 0.01$), and fat depot (0.71; $p < 0.01$) are highlighted in **bold**. These relationships are illustrated in Figs. 2, 3, & 5

Explanatory variable	CSL EOF 1	CSL EOF 2	Fat depot
SST EOF 1	0.21	0.46	0.49
SST EOF 2	0.11	**0.73**	0.21
Anchovy EOF 1	–0.41	0.01	0.37
Anchovy EOF 2	0.07	0.56	–0.12
Sardine EOF 1	0.20	–0.35	0.17
Sardine EOF 2	**0.75**	0.36	**0.71**

and false negative (FN) values mean that the model incorrectly predicted presence or absence of an actual sea lion. Because the sea lion tracking data have reduced spatial coverage compared to the IBM (i.e. 18, 3, and 10 animals were respectively tagged in 2003-04, 2004-05, and 2005-06 compared to 1000 model individuals followed each year), the binary discriminator test was performed on a 0.5° × 0.5° grid, which is roughly equivalent to evaluating the ability of the model to predict the presence or absence of an actual sea lion within a ca. 25 km radius. Finally, because sea lion behavior in the IBM is cued on SST, model–data correspondence was also evaluated by comparing the temperatures experienced by simulated sea lion individuals against satellite SST measurements extracted along the observed sea lion tracks.

RESULTS

Foraging patterns

The first EOF mode for annual sea lion abundances explained 66% of the total variance and correlated most strongly (r = 0.75) with the second EOF mode for annual sardine population abundances (Table 1). The spatial and temporal variability associated with the first mode primarily identified coast-wide changes in foraging patterns (although some variability was also present at the scale of individual haul-out locations in the northern half of the domain) in response to fluctuations in sardine abundance off of central California (Fig. 2). The correlation between the sea lion and sardine EOF modes suggests that sea lions spent less time foraging at sea (i.e. reduced abundance owing to fewer individuals being present) during periods of increased sardine presence nearshore, as evidenced by the region of negative sea lion abundance anomalies (Fig. 2, left panel) corresponding to the region of positive sardine abundance anomalies (Fig. 2, right panel). This relationship can be further tied to the occurrence of coherent positive SST anomalies over the entire CCLME region (viz. first EOF mode and domain-wide annual mean values in Figs. S2 & S3), which is known to correlate strongly with the PDO (Fiechter et al. 2015).

The second EOF mode for annual sea lion abundances explained 13% of the total variance and was most strongly related (r = 0.73) to the second EOF mode for annual mean SST (Table 1). The spatial and temporal variability associated with the second mode isolated foraging variability that was either coastal along most of central California (i.e. between 35 and

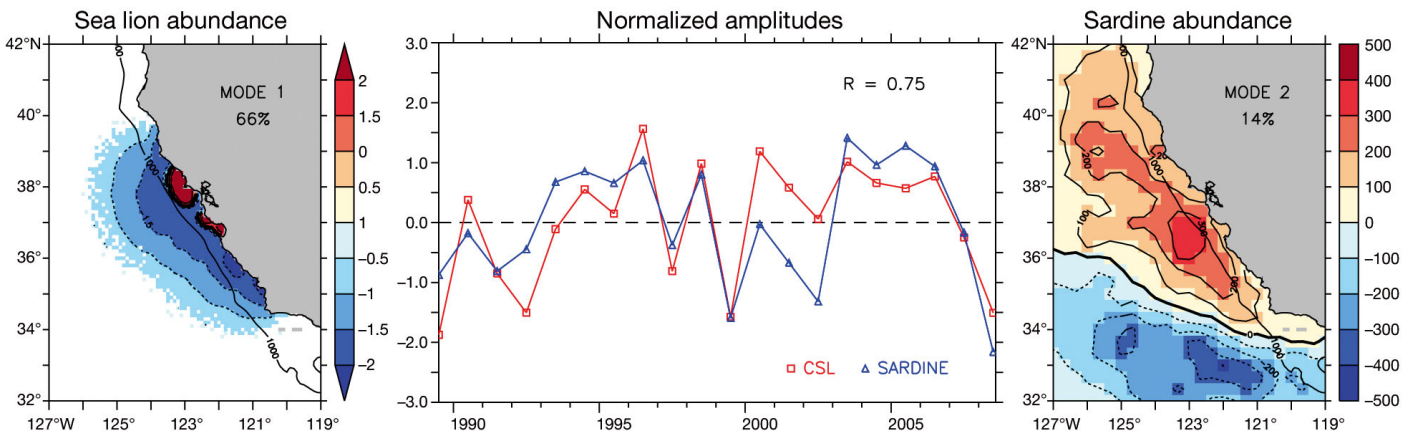

Fig. 2. Coast-wide foraging variability. First empirical orthogonal function (EOF) mode for California sea lion (CSL) abundance (log_{10}[individuals]) and the second EOF mode for sardine abundance (millions of individuals). Left and right: spatial patterns and percent variance explained. Center: normalized annual amplitudes

38° N) or offshore and near the northern ends of the simulated range (Fig. 3). Based on the EOF time amplitude, sea lion individuals favored more offshore and northern locations during the early and mid-1990s, but switched to more coastal foraging from 1999 on. During the second half of the simulation period, 2005 also emerged as a strongly anomalous year during which sea lion foraging patterns switched from nearshore to offshore. The relationship between onshore–offshore sea lion abundance and coastal SST indicated that spatial changes in foraging patterns were primarily linked to upwelling variability off of central California. Foraging occurred preferentially nearshore during years of strong upwelling and farther offshore during anomalously warm conditions (i.e. 1992-93, 1998, and 2005), as evidenced by the region of positive sea lion abundance anomalies offshore (Fig. 3, left panel) during years of positive coastal SST anomalies (Fig. 2, right panel). The link between coastal upwelling intensity and the second EOF mode for SST is further evidenced by its strong correlation (r = 0.76) with periods of decreased nearshore vertical velocities (i.e. a measure of upwelling transport) off of central California (Fig. S3). The spatial and temporal SST patterns associated with this particular EOF mode (i.e. upwelling variability off central California) are known to correlate, albeit weakly, with the El Niño 3.4 index and Bakun upwelling index (Fiechter et al. 2015).

A direct comparison between model output and tracking data acquired in 2003 to 2006 further illustrated the significant offshore shift in sea lion distribution. Tracks in 2004 displayed mainly nearshore foraging along the entire central California coast, tracks in 2005 exhibited substantial offshore foraging at most latitudes, and tracks in 2006 revealed an intermediate pattern where sea lions foraged nearshore in the southern half of the domain (34.5–36.5° N) but ventured farther offshore in the northern half (36.5–39° N; Fig. 4, top panels). Average temperatures experienced by sea lion individuals in the model were also consistent with remotely-sensed SSTs extracted along observed animal tracks, which confirmed that simulated distributions were representative of expected shifts in sea lion foraging patterns in response to changes in coastal ocean temperatures off of central California (Fig. 4, bottom panel).

The agreement between simulated and observed foraging locations was quantified by determining predictive values for presence and absence. The binary discriminator test indicated that for 2004 the model overestimated the offshore extent of foraging locations along most of the central California coast (Fig. 5, left panel). In contrast, for 2005 and 2006, the model overestimated foraging locations in the southern and northern parts of the domain, and underestimated them in the central region (Fig. 5, center and right panels). Nevertheless, the model exhibited reasonable overall skill with a combined predictive value of ca. 70% for each year over the region considered, although simulated foraging locations better reproduced absence in 2004 (APV of 0.89) and presence in 2005 and 2006 (PPV of 0.79 and 0.7, respectively).

Foraging success

Based on the annual EOF amplitudes for SST and prey availability (i.e. sardine and anchovy abundances), annual variation in fat depot correlated most

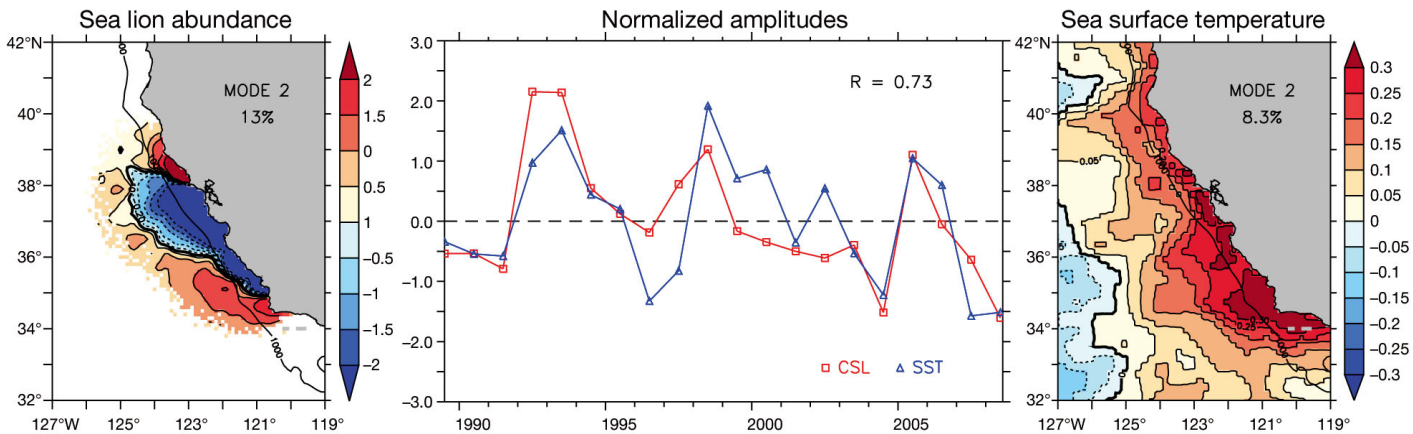

Fig. 3. Onshore–offshore foraging variability. Second empirical orthogonal function (EOF) mode for California sea lion abundnce (log_{10}[individuals]) and second EOF mode for sea surface temperature (SST, °C). Left and right: spatial patterns and percent variance explained. Center: normalized annual amplitudes

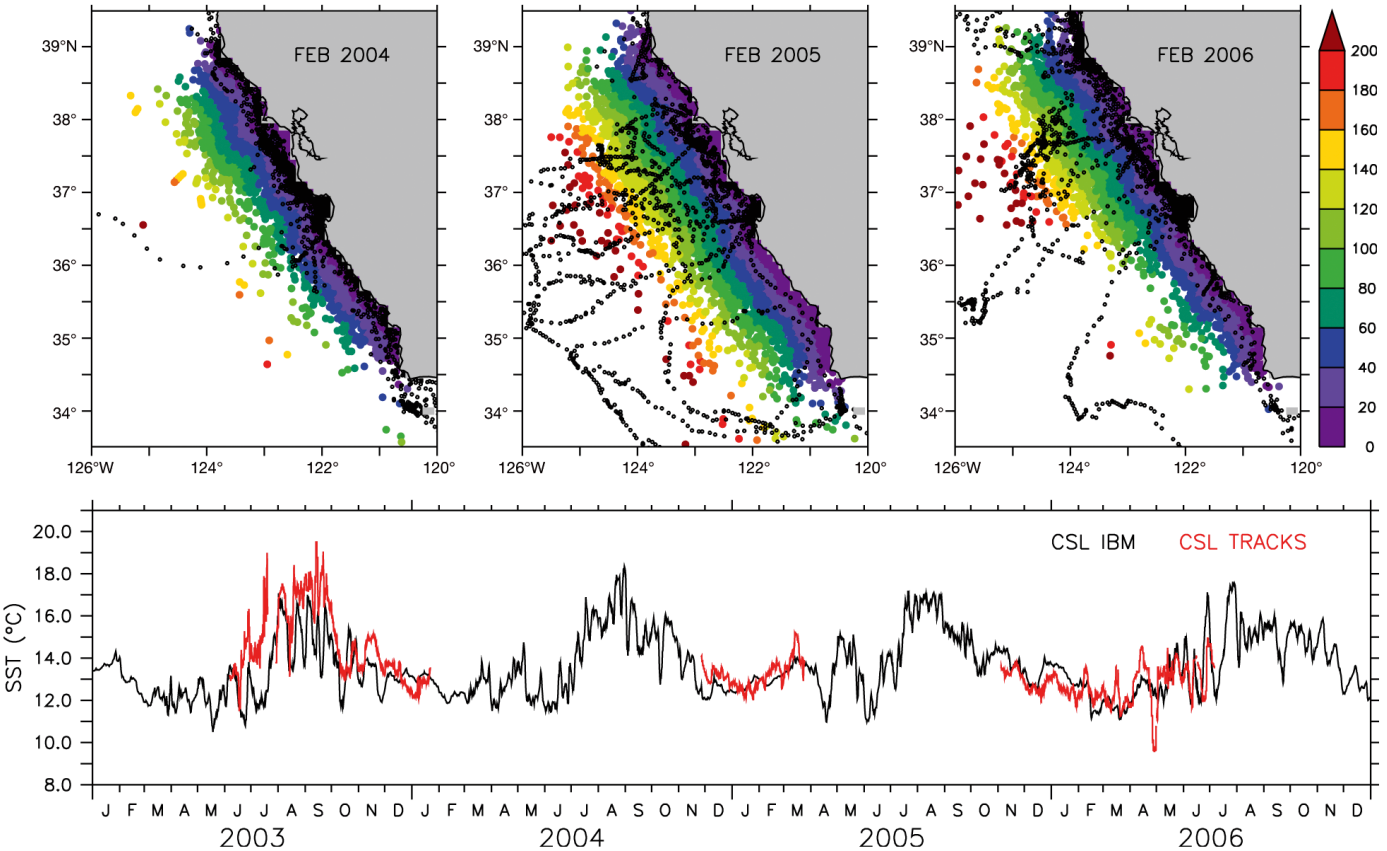

Fig. 4. Model–data comparison. Top: simulated (colored circles) and observed (black circles) foraging locations for male California sea lion (CSL) individuals off of central California in 2004 (left), 2005 (center), and 2006 (right); simulated locations are for February and color scale represents offshore distance (km); observed locations are based on tracking data collected during winter (November to March) of 2003-2004, 2004-2005, and 2005-2006. Bottom: mean sea surface temperature (SST, °C) experienced by model individuals (black) and tagged animals (red) during 2003–2006

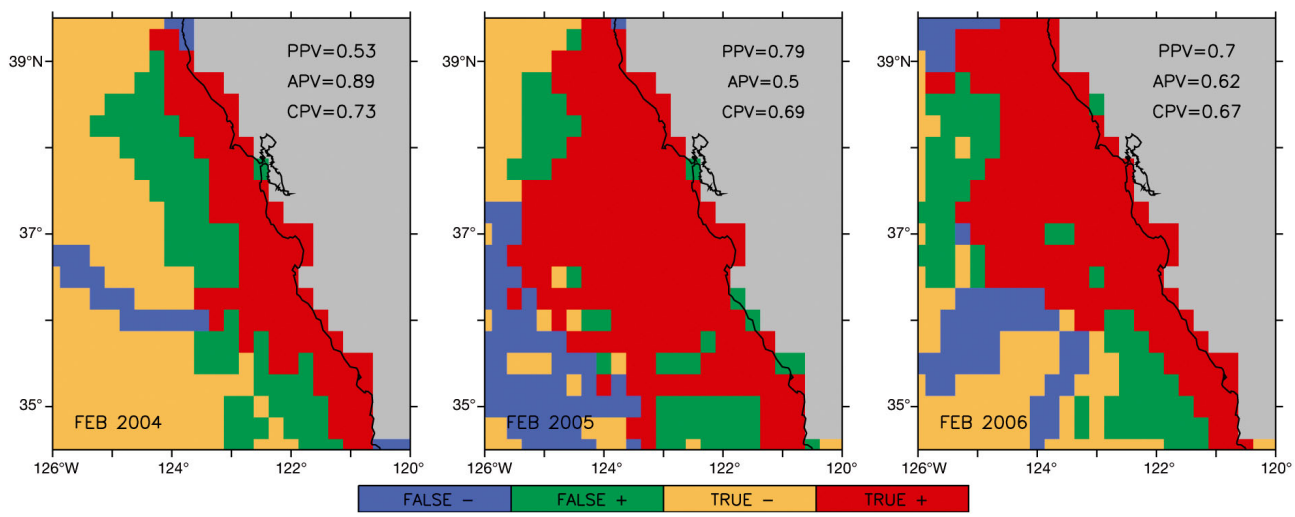

Fig. 5. Model predictive skill. Simulated vs. observed locations where California sea lions were present or absent in 2004 (left), 2005 (center), and 2006 (right). Red and yellow indicate locations where the model correctly predicted presence (i.e. true positive) and absence (i.e. true negative), respectively. Green and blue indicate locations where the model incorrectly predicted presence (i.e. false positive) and absence (i.e. false negative), respectively. Model skill is quantified as presence predictive value (PPV), absence predictive value (APV), and combined predictive value (CPV) (see 'Methods' for definitions)

strongly (0.71) with the second mode for sardine abundance (i.e. the mode associated with coast-wide changes in foraging patterns; Table 1 and Fig. 6, top panel). While sardine typically accounted for a smaller fraction of the sea lion diet than anchovy (4.4 vs. 8.4 kg d^{-1}), relative changes in annual sardine consumption were, on average, twice as large (standard deviation relative to the mean of 11 versus 6%; Fig. 6, middle panel). As sardine have a higher energy density (7.3 kJ g^{-1}) than the alternative prey of anchovy (6.6 kJ g^{-1}), market squid (4.4 kJ g^{-1}), and mackerel (6.4 kJ g^{-1}), the ability for sea lions to accumulate fat was particularly hindered during years when sardine abundance was substantially reduced in the simulation (i.e. 1991 and 1999).

In addition to decreasing energy content in the diet, lower sardine abundance also resulted in sea lions extending the duration of their foraging trips in order to fulfill their daily food requirement (as indicated by the first EOF mode for foraging patterns in Fig. 2). Since the end of a foraging trip in the model is triggered when the body mass lost while hauled out has been regained, sea lion individuals can recover weight faster if sardines are present nearshore (i.e. higher energy content in diet) compared to instances when anchovy are the more dominant prey source.

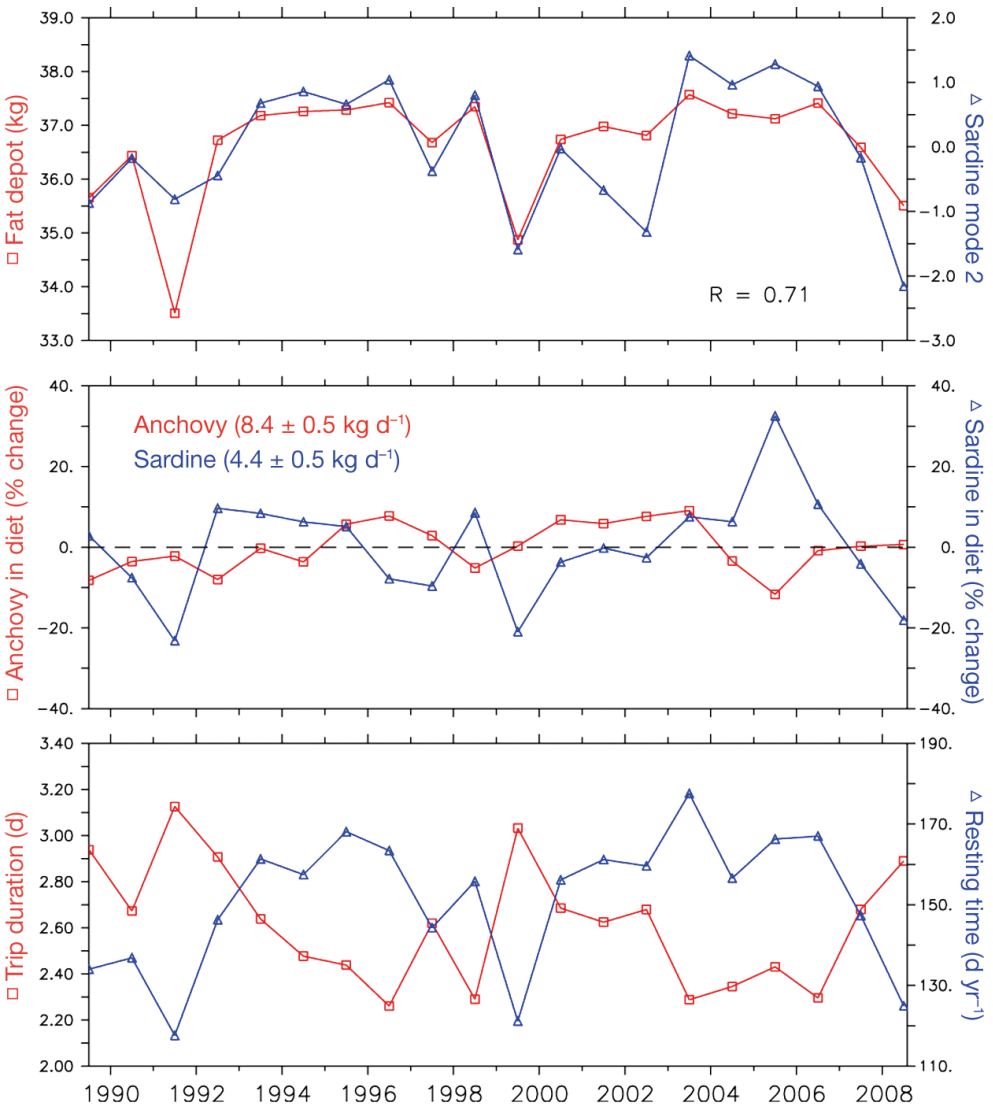

Fig. 6. Foraging success and diet composition. Top: annual mean California sea lion fat depot (kg) (left *y*-axis and red squares) and the normalized annual amplitude of the second empirical orthogonal function (EOF) mode for sardine abundance (right *y*-axis and blue triangles). Middle: relative change of annually averaged anchovy (left *y*-axis and red squares) and sardine (right *y*-axis and blue triangles) contributions to sea lion diet with respect to 20 yr mean. Bottom: annual mean sea lion foraging trip duration (d; left *y*-axis and red squares) and time spent on land (d yr^{-1}; right *y*-axis and blue triangles)

Hence, the average trip duration of individuals increased substantially during periods of sardine scarcity off of central California, which translated to shorter resting times on land and the number of haul-out days per year dropping by roughly 20% (ca. 120 d in 1991 and 1999 vs. 150 d on average; Fig. 6, bottom panel). In 1991 and 1999, sea lion individuals also reached the limit of 3 d allowed for trip duration in the model, implying that foraging success was typically insufficient to achieve optimal growth for these particular years.

Considering the inherent variability in the actual apportion of sardine and anchovy in the diet of California sea lions, the bioenergetics component of the IBM was used to determine the robustness of the results to a range of diet compositions around the baseline values of 33% for anchovy and 17% for sardine. For a fixed sardine fraction, decreasing (increasing) the biomass of anchovy consumed has the effect of amplifying (dampening) interannual fluctuation in fat depot (Fig. S4, top left panel). With the current parameterization, the results suggest that if the anchovy diet contribution falls to 5%, individuals no longer survive years of low sardine abundance. Year-to-year changes in fat depot are similarly amplified (dampened) when sardine consumption is increased (decreased) given a fixed anchovy fraction (Fig. S4, top right panel). At 50% apportion, individuals are no longer able to sustain body mass during years of low sardine abundance. An additional simulation of the fully coupled model was also performed to determine sensitivity to the diet fraction contributed by market squid and mackerel. When the relative contributions of the 2 species are allowed to vary annually instead of being fixed to the long-term mean (Fig. S5), the results suggested that a shift toward a higher abundance of squid (a lower energy density prey) with respect to mackerel (a higher energy density prey) decreases the ability of sea lions to cope with poorer foraging during periods of unfavorable environmental conditions and limited sardine and anchovy availability, as evidenced by larger losses in fat depot (Fig. S6).

As the ability of sea lions to fulfill their intake needs in the model also depends on time spent feeding at sea, the sensitivity analysis was extended to the parameters controlling foraging trip and haul-out durations. Although fat depot is relatively insensitive to minimum foraging duration, the results suggest that, not unexpectedly, increasing maximum trip duration and reducing haul-out interval help sea lion individuals cope during years of poorer feeding conditions (Fig. S4, lower panels).

DISCUSSION

Despite simplifications to the full array of physical and biological processes influencing bioenergetics and behavior, the fully coupled ecosystem model provides a comprehensive framework to unravel the complex interplay between environmental variability, prey availability, and the foraging ecology of California sea lions in the CCLME. For example, using a simple temperature cue in the model to represent foraging behavior was sufficient for onshore–offshore shifts in sea lion distributions to emerge within the simulation as a dominant mode of variability. However, while satellite tracking observations available for 2003–2006 were critical to evaluate whether the model reproduced onshore–offshore shifts in foraging behavior, the necessarily limited spatial and temporal resolution of the observations precludes an assessment of the full range of interannual variability that is captured in the 20 yr simulation. Based on the 1989–2008 period, the model results identify potential environmentally and prey-mediated impacts on the foraging ecology of sea lions off of central California, with connections to the PDO via increased sardine abundance nearshore and to ENSO via modulation of coastal upwelling intensity. The relationship between positive temperature anomalies, increased nearshore sardine abundances, and improved sea lion foraging success that emerged from the simulation is also generally consistent with population surveys suggesting higher sea lion abundances off of central California during warmer ocean conditions (e.g. El Niño years) in response to better feeding conditions (Sydeman & Allen 1999, Lowry & Forney 2005).

While the model was parameterized to roughly reproduce existing historical (1981–1995) diet composition for sea lions off of southern California (Lowry & Carretta 1999), the data correspond to a period during which the abundances of anchovy and jack mackerel were relatively high and those of sardine and market squid were relatively low. In contrast, more recent information corresponding to a period of lower population abundances for sardine and anchovy suggests that the 2 species contributed less than 20% to diet composition (Hassrick et al. 2014, McClatchie et al. 2016). Variability in prey importance might be further compounded by 'extreme' events, as evidenced by data from Monterey Bay (i.e. at the center of the foraging range considered here) suggesting that during the 1997–98 El Niño and 1999 La Niña, sardine contributed about half of the total biomass consumed by sea lions, whereas anchovy, market squid, and mackerel individually accounted

for less than 10% (Weise & Harvey 2008). While an increase in sardine in the diet also occurs in the model in 1998, the substantial decrease in 1999 does not seem consistent with the observations. This discrepancy could stem from a potential behavior mismatch in the model, where the temperature cues imposed for sea lion and sardine movement increased encounter rates during warmer years (e.g. 1998) by allowing sardine to move onshore, but limited too severely the overlap of their spatial distributions during colder years (e.g. 1999) by forcing sea lions closer to shore and constraining sardine to offshore waters.

The behavioral component of the IBM is expected to carry a significant amount of uncertainty in general since very little information exists to determine the exact cues that sea lions rely on for foraging (as opposed to the bioenergetics component which can be more solidly grounded using existing laboratory data). For example, the tolerance around optimal conditions used in kinesis to bias movement towards inertial or random behavior can substantially alter simulated foraging distributions and result in model–data discrepancies such as those identified with the binary discriminator test for 2004, 2005, and 2006. Using a single cue (i.e. temperature) for behavior is also likely to influence habitat selection and may in part explain the model overestimating offshore foraging distance in 2004 (e.g. sea lions in the wild may use topographic cues to concentrate their foraging in nearshore waters when conditions are favorable there). However, because little is known about actual foraging cues used by sea lions, the model was intentionally kept simple to avoid imposing rules that would constrain movement too strictly.

While the bioenergetics and behavioral components implemented in the IBM can always be improved in the future, the current model framework is sufficiently evolved to determine the impact of long-term changes in prey assemblage on sea lion foraging ecology off of central California. For example, a diet sensitivity analysis performed with the model confirmed that interannual variability in fat depot is significantly influenced by sardine consumption, yet it also indicated that changes in the absolute and relative fractions of sardine and anchovy biomasses ingested may enhance or mitigate the ability of the sea lions to accumulate fat during poorer feeding conditions. These effects are also further compounded by fluctuations in the full prey assemblage available to sea lions during any particular year (e.g. higher relative abundance of mackerel vs. squid may help sea lions cope with decreased sardine availability).

Another important aspect of the results presented here is that, because behavioral cues are specified *a priori* in the model, overlap of habitat preferences between prey and predator species can be easily determined. This information in turn provides a means to characterize potential 'hotspots' (defined here as spatiotemporal regions exploited for foraging by species over multiple trophic levels), a topic to which much attention has been recently devoted with the increased availability of satellite tagging data for a wide range of marine organisms (e.g. Bailey et al. 2009, Hazen et al. 2012). While determining preferred habitat features based on observed animal tracks typically requires isolating foraging vs. transiting behavior, 'hotspots' are readily identifiable in the model solution by considering regions where both prey and predator individuals favored inertial behavior in kinesis (i.e. an indication of near optimal environmental and feeding conditions). To illustrate this point, the IBM results were used to produce habitat preference maps describing seasonal and annual mean locations where optimal conditions overlapped for sardine, anchovy, and sea lions, and were therefore conducive to biomass aggregation over multiple trophic levels (Fig. 7). It is worth noting that the maps reveal a remarkable amount of intra-annual variability, with optimal conditions present mainly offshore during winter and limited to a narrow nearshore region during summer. While the actual existence of these seasonal 'hotspots' is rather difficult to validate, there are noticeable similarities between the model results and observed sea lion foraging locations identified using a state–space model (Jonsen et al. 2005) applied to the 2003–2006 tracking data (e.g. most observed foraging locations fall within the region of preferred conditions derived from the simulation).

In a broader context, the results illustrate the benefits of using an integrated ecosystem modeling framework that explicitly resolves the spatial and temporal scales at which environmental variability and forage base dynamics impact the distribution and feeding success of their predators. As such, the fully coupled simulations described here belong to an emerging class of 'end-to-end' ecosystem models that attempt to replicate environmental and food web dynamics (and human impacts) in a way that allows for a more direct understanding of the complex physical and biological interplay determining the distribution and abundance of marine organisms from primary and secondary producers to forage fish species and, ultimately, to apex predators (Rose et al. 2010, Holt et al. 2014). Combined with recent advances in animal tagging (Block et al. 2011), these models have

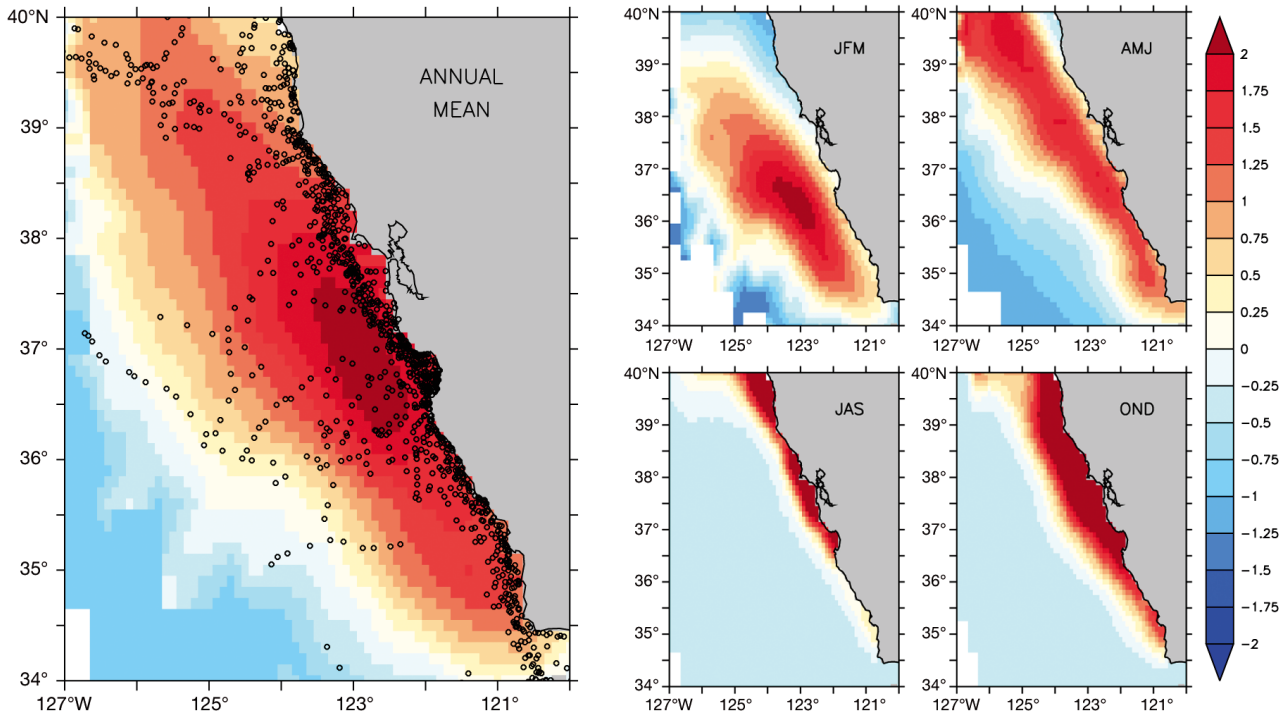

Fig. 7. Simulated (color maps) and observed (black circles) preferred foraging locations of California sea lions. Left: annual mean. Right: seasonal means for January to March (JFM), April to June (AMJ), July to September (JAS), and October to December (OND). Simulated foraging preferences are based on combined optimal behavior conditions (standardized) for sardine, anchovy, and sea lions; warm (cool) colors denote above (below) average conditions. Observed foraging locations are calculated using a state space model applied to sea lion along-track behavior

the potential, as demonstrated here, to identify the physical and biological mechanisms through which changing environmental and climate conditions will likely impact the foraging ecology of marine organisms at local and regional scales and over multiple trophic levels.

Acknowledgements. This research was funded by the Office of Naval Research Marine Mammals and Biology Program (grant N000141210893). We also acknowledge Enrique Curchitser, Christopher Edwards, and Katherine Hedstrom for their contributions to the development and implementation of the ecosystem model.

LITERATURE CITED

Bailey H, Mate BR, Palacios DM, Irvine L, Bograd SJ, Costa DP (2009) Behavioural estimation of blue whale movements in the Northeast Pacific from state-space model analysis of satellite tracks. Endang Species Res 10: 93–106

Bakun A (2006) Wasp-waist populations and marine ecosystem dynamics: navigating the 'predator pit' topographies. Prog Oceanogr 68:271–288

Block BA, Jonsen ID, Jorgensen SJ, Winship AJ and others (2011) Tracking apex marine predator movements in a dynamic ocean. Nature 475:86–90

Brink KH, Cowles TJ (1991) The coastal transition zone program. J Geophys Res 96:14637–14647

Carretta JV, Forney KA, Muto MM, Barlow J, Baker J, Hansen B, Lowry MS (2005) U.S. marine mammal stock assessments: 2004. NOAA Tech Memo NMFS NOAA-TM-NMFS-SWFSC-375. National Marine Fisheries Service, La Jolla, CA

Carton JA, Chepurin G, Cao X (2000) A Simple Ocean Data Assimilation analysis of the global upper ocean 1950–1995. Part 2: results. J Phys Oceanogr 30:311–326

Conkright ME, Boyer TP (2002) World ocean atlas 2001: objective analyses, data statistics, and figures. CD-ROM Documentation, National Oceanographic Data Center, Silver Spring, MD

Di Lorenzo E, Schneider N, Cobb KM, Franks PJS and others (2008) North Pacific Gyre Oscillation links ocean climate and ecosystem change. Geophys Res Lett 35:L08607

Fiechter J, Rose KA, Curchitser EN, Hedstrom K (2015) The role of environmental controls in determining sardine and anchovy population cycles in the California Current: analysis of an end-to-end model. Prog Oceanogr 138: 381–398

Fiedler PC, Reilly SB, Hewitt RP, Demer D, Philbrick VA, Smith S, Mate BR (1998) Blue whale habitat and prey in the California Channel Islands. Deep-Sea Res II 45: 1781–1801

Field JC, Francis RC, Aydin K (2006) Top-down modeling and bottom-up dynamics: linking a fisheries-based ecosystem model with climate hypotheses in the northern California Current. Prog Oceanogr 68:238–270

Haidvogel DB, Arango H, Budgell WP, Cornuelle BD and others (2008) Ocean forecasting in terrain-following coordinates: formulation and skill assessment of the Regional Ocean Modeling System. J Comput Phys 227:3595–3624

Hassrick J, Robinson H, Hernandez K, Morris P, Thayer J, Weise M (2014) Temporal variation in California sea lion food habits: 2010 and 2013. Farallon Institute Technical Report. www.faralloninstitute.org/publications.php

Hazen EL, Jorgensen S, Rykaczewski RR, Bograd SJ and others (2013) Predicted habitat shifts of Pacific top predators in a changing climate. Nature Climate Change 3: 234–238

Holt J, Allen JI, Anderson TR, Brewin R and others (2014) Challenges in integrative approaches to modelling the marine ecosystems of the North Atlantic: physics to fish and coasts to ocean. Prog Oceanogr 129:285–313

Humston R, Olson DB, Ault JS (2004) Behavioral assumptions in models of fish movement and their influence on population dynamics. Trans Am Fish Soc 133:1304–1328

Irvine LM, Mate BR, Winsor MH, Palacios DM, Bograd SJ, Costa DP, Bailey H (2014) Spatial and temporal occurrence of blue whales off the U.S. West Coast, with implications for management. PLOS ONE 9:e102959

Jonsen ID, Flemming JM, Myers RA (2005) Robust state–space modeling of animal movement data. Ecology 86: 2874–2880

Kastelein RA, Schooneman NM, Vaughan N, Wiepkema PR (2000) Food consumption and growth of California sea lions (*Zalophus californianus californianus*). Zoo Biol 19: 143–159

Kishi MJ, Kashiwai M, Ware DM, Megrey BA and others (2007) NEMURO — a lower trophic level model for the North Pacific marine ecosystem. Ecol Model 202:12–25

Kosro PM, Huyer A, Ramp SR, Smith RL and others (1991) The structure of the transition zone between coastal waters and the open ocean off northern California, winter and spring 1987. J GeophysRes 96:14707–14730

Large WG, Yeager SG (2009) The global climatology of an interannually varying air–sea flux data set. Clim Dyn 33: 341–364

Lavigne DM, Innes S, Worthy GAJ, Kovacs KM (1986) Metabolic rate — body size relations in marine mammals. J Theor Biol 122:123–124

Lowry MS, Carretta JV (1999) Market squid (*Loligo opalescens*) in the diet of California sea lions (*Zalophus californianus*) in southern California (1981–1995). Calif Coop Ocean Fish Invest Rep 40:196–207

Lowry MS, Forney KA (2005) Abundance and distribution of California sea lions (*Zalophus californianus*) in central and northern California during 1998 and summer 1999. Fish Bull 103:331–343

Lynn RJ, Bograd SJ (2002) Dynamic evolution of the 1997–1999 El-Niño – La-Niña cycle in the southern California Current System. Prog Oceanogr 54:59–75

Mantua NJ, Hare SR, Zhang Y, Wallace JM, Francis RC (1997) A Pacific interdecadal climate oscillation with impacts on salmon production. Bull Am Meteorol Soc 78: 1069–1079

McClatchie S, Field J, Thompson AR, Gerrodette T and others (2016) Food limitation of sea lion pups and the decline of forage off central and southern California. R Soc Open Sci 3:150628

Palacios DM, Bograd SJ, Foley DG, Schwing FB (2006) Oceanographic characteristics of biological hot spots in the North Pacific: a remote sensing perspective. Deep-Sea Res II 53:250–269

Rose KA, Allen JI, Artioli Y, Barange M and others (2010) End-to-end models for the analysis of marine ecosystems: challenges, issues, and next steps. Mar Coast Fish 2:115–130

Rose KA, Fiechter J, Curchitser EN, Hedstrom K and others (2015) Demonstration of a fully-coupled end-to-end model for small pelagic fish using sardine and anchovy in the California Current. Prog Oceanogr 138:348–380

Rykaczewski RR, Checkley DM Jr (2008) Influence of ocean winds on the pelagic ecosystem in upwelling regions. Proc Natl Acad Sci USA 105:1965–1970

Scheffer M, Baveco JM, DeAngelis DL, Rose KA, van Nes EH (1995) Super-individuals a simple solution for modelling large populations on an individual basis. Ecol Model 80:161–170

Schwartzlose RA, Alheit J, Bakun A, Baumgartner TR and others (1999) Worldwide large-scale fluctuations of sardine and anchovy populations. S Afr J Mar Sci 21:289–347

Shchepetkin AF, McWilliams JC (2005) The regional oceanic modeling system (ROMS): a split-explicit, free-surface, topography-following-coordinate oceanic model. Ocean Model 9:347–404

Stow CA, Jolliff J, McGillicuddy DJ Jr, Doney SC and others (2009) Skill assessment for coupled biological/physical models of marine systems. J Mar Syst 76:4–15

Sydeman WJ, Allen SG (1999) Pinniped population dynamics in central California: correlations with sea surface temperature and upwelling indices. Mar Mamm Sci 15: 446–461

Thomson RE, Emery WJ (2014) Data analysis methods in physical oceanography, 3rd edn. Elsevier, Waltham, MA

Weise MJ, Harvey JT (2008) Temporal variability in ocean climate and California sea lion diet and biomass consumption: implications for fisheries management. Mar Ecol Prog Ser 373:157–172

Weise MJ, Costa DP, Kudela RM (2006) Movement and diving behavior of male California sea lion (*Zalophus californianus*) during anomalous oceanographic conditions of 2005 compared to those of 2004. Geophys Res Lett 33: L22S10

Editorial responsibility: Peter Corkeron, Woods Hole, Massachusetts, USA

Submitted: January 29, 2016; Accepted: July 25, 2016
Proofs received from author(s): August 22, 2016